

# Chemical composition, structural properties, rheological behavior and functionality of *Melissa officinalis* seed gum

Mohebbat Mohebbi<sup>a,\*</sup>, Morteza Fathi<sup>b</sup>, Mohammad Khalilian-Movahhed<sup>a</sup>

<sup>a</sup> Department of Food Science and Technology, Ferdowsi University of Mashhad, Mashhad, Iran

<sup>b</sup> Department of Food Science, Engineering and Technology, Campus of Agriculture and Natural Resources, University of Tehran, Karaj, Iran

## ARTICLE INFO

### Keywords:

*Melissa officinalis* seed Gum  
Chemical composition  
Structural characteristics  
Anti-oxidative capacity

## ABSTRACT

In the present work, the chemical composition, structural properties, rheological behavior and biological activity of a novel polysaccharide extracted from *Melissa officinalis* seeds were examined. *Melissa officinalis* seed gum (MOSG) is mainly composed of galactose and mannose. The weight average molecular weight of MOSG was found to be  $1.36 \times 10^7$  g/mol. The zeta potential of MOSG was  $-44.26 \pm 0.67$  mV (at pH = 7). A time-dependent and strong shear-thinning behavior was observed for MOSG dispersions at different concentrations (0.5, 1 and 1.5% (w/w)). The intrinsic viscosity of MOSG was 3.45 dL/g. MOSG could effectively scavenge free radicals with certain dose-effect relationships. MOSG can be employed as gelling agent, stabilizer and antioxidant in food, cosmetic and pharmaceutical systems.

## 1. Introduction

Gums are widely employed in commercial salad dressings to improve the quality of food products such as sensory attributes. Furthermore, gums and mucilages can be used as flavoring agent (Andres, Von Düring, Muszynski & Schmidt, 1987). Due to recent concern related to the application of synthetic polymers in food products, the search for finding new sources of natural polymers has attracted the attention of researchers (Buera et al, 2018; Dokht et al, 2018; Hesarinejad et al 2015; Razavi et al, 2014; Koocheki, 2015; Wang et al, 2015).

*Melissa officinalis* plant belongs to Lamiaceae family. This plant is mainly distributed in south-central Europe, the Mediterranean Basin, Iran, and Central Asia. In Austrian, the oils extracted from *M. officinalis* leaves are used to treat disorders of the gastrointestinal tract, nervous system, liver, and bile. Furthermore, in alternative medicine, this plant is used as a sleep aid and digestive aid (Vogl et al., 2013).

The functional properties of biopolymers such as antioxidant activity, thickening and gelling abilities, and stabilizing properties are mainly dependent on their physico-chemical and structural characteristics. Hence, the present work was undertaken to investigate the chemical composition, structural characteristics as well as rheological and functional properties of the gum extracted from the seeds of *Melissa officinalis* to predict its potential applications in food, pharmaceutical and textile industries.

## 2. Materials and methods

### 2.1. Materials

*Melissa officinalis* seeds were purchased from a local market in Mashhad, Iran. The reagents and chemicals were obtained from Sigma Aldrich Co (Sigma-Aldrich Co. St Louis, MO, USA).

### 2.2. Gum extraction and purification

The extraction of MOSG was carried out using deionized water at different extraction conditions. The preliminary tests exhibited that the gum extracted at temperature of 65 °C and pH 7 (at constant extraction time of 30 min) had maximum extraction yield (16.9%). For purification of MOSG, 100 g of collected gum was submitted to aqueous extraction, with 1000 mL deionized water. The resulting dispersion was filtrated and then precipitated by 95% ethanol with respective ratio of 1:4 (v/v). Afterward, centrifugation was conducted at 3000 g for 10 min to collect the precipitates. The precipitate was de-proteinized by Sevag assay. Then, it was again dispersed in deionized water, and centrifuged at 300 g (5 min) to remove bubbles and insoluble materials. Finally, the dispersion was lyophilized and stored in a desiccator at 25 °C until further experiments.

\* Corresponding author.

E-mail address: [m-mohebbi@um.ac.ir](mailto:m-mohebbi@um.ac.ir) (M. Mohebbi).

<https://doi.org/10.1016/j.bcdf.2022.100315>

Received 21 August 2021; Received in revised form 3 January 2022; Accepted 24 January 2022

Available online 24 February 2022

2212-6198/© 2022 Elsevier Ltd. All rights reserved.

## 2.3. Chemical composition

### 2.3.1. General analysis methods

The amount of protein in MOSG composition was determined based on Bradford method (Bradford, 1976), with bovine serum albumin as standard. The amounts of moisture, fat, and ash in MOSG were quantified based on the standard methods of AOAC (International, 2005).

The phenol-sulfuric acid colorimetric assay with use of galactose as standard, was used to determine the total carbohydrate content. Uronic acid content was determined by carbazole method using D-galactose as standard (Brunner & Cui, 2005).

Folin Ciocalteu spectrophotometric assay was employed to determine total phenol content of MOSG (Singleton & Rossi, 1965). For this purpose, first, 0.5 mL of MOSG solution was added to 2.5 mL of 0.2 N Folin-Ciocalteu reagent and stored at 25 °C for 5 min. Afterward, 2.0 mL of 75 g/L Na<sub>2</sub>CO<sub>3</sub> was mixed with the resulting solution and allowed to stand at 25 °C for 1 h. Finally, the absorbance of the prepared solutions was read at 760 nm using a UV/Visible spectrophotometer. The results were expressed as mg gallic acid/100 g of the samples.

### 2.3.2. Monosaccharide determination

MOSG was hydrolyzed with 2 M trifluoroacetic acid (TFA) for 8 h at 100 °C and then subjected to microwave. The resulting reaction mixture was reduced by sodium borohydride, followed by addition of anhydride and pyridine with a ratio of 10:1 (Wolfrom & Thompson, 1963). Finally, the resulting mixture was incubated at 100 °C for 20 min to acetylate the alditols. An Agilent gas chromatography (GC) equipped a mass spectroscopy (MS) was employed to detect the monosaccharides. HP-5MS capillary column was used for this purpose. The experiment conditions were as follow: Flow rate of carrier gas (helium) was kept at 1.2 mL min<sup>-1</sup>. The chromatographic oven was held at 120 °C for 1 min, followed by raising to 300 °C at a constant rate of 6 °C.min<sup>-1</sup>. Finally, the temperature kept at 300 °C for 15 min.

### 2.3.3. Mineral analysis

Mineral profile of MOSG was determined using inductively coupled plasma optical emission spectrometry (ICP-OES, PerkinElmer, Waltham, MA, U.S.A.) with a cross-flow nebulizer. The gum sample was digested in a mixture solution of HNO<sub>3</sub> and HClO<sub>4</sub> with a respective ratio of 4:1, w/w.

### 2.3.4. FT-IR analysis

The organic functional groups of MOSG were identified by a Fourier Transform Infrared (FT-IR) spectrometer (PerkinElmer). The analysis was conducted in the frequency range of 400–4000 cm<sup>-1</sup>. The resolution of device was 4 cm<sup>-1</sup>.

### 2.3.5. Nuclear magnetic resonance (NMR) analysis

The gum sample (30 mg) was dissolved in 0.5 mL of D<sub>2</sub>O and subjected to <sup>13</sup>C NMR evaluation. NMR spectrum of MOSG was scanned using a Bruker AVANCE III HD 400 MHz NMR spectrometer (Bruker, Germany) at 298 K.

## 2.4. Antioxidant capacity

The ability of MOSG solutions to scavenger free radicals was evaluated according to the earlier reported assay (Blois, 1958) with slight adjustments. 0.5 mL of methanolic α, α-diphenyl-β-picrylhydrazyl (DPPH) solution (0.1 mM) was incorporated into 3 mL of MOSG solutions with different concentrations. Then, the mixtures were vigorously shaken, and incubated for 30 min at 37 °C. Finally, the changes in absorbance of the solutions were recorded by a UV-VIS spectrophotometer (Shimadzu, Kyoto, Japan) at 517 nm.

The scavenging activity of the gum solutions was quantified using the following equation:

$$\% \text{inhibition} = \frac{A_{\text{Control}} - A_{\text{Sample}}}{A_{\text{Sample}}} \times 100 \quad \text{Eq. 1}$$

here,  $A_{\text{Control}}$  and  $A_{\text{Sample}}$  are the absorbance read for the control and gum solutions, respectively.

## 2.5. Rheological behavior

### 2.5.1. Sample preparation

MOSG solutions were prepared by dispersing specific amounts of gum powder in deionized water on a magnetic stirrer at ambient temperature (23 ± 2 °C). Then, the dispersions were kept at refrigerator for overnight to be hydrated completely before further assessments.

### 2.5.2. Dilute solution properties

The dilute solution behavior of MOSG solutions was evaluated using Ubbelohde capillary viscometer (Cannon Instruments Co., USA), equipped with a water bath to control temperature.

Huggins equation was used to determine the intrinsic viscosity of MOSG (Huang, Kakuda, & Cui, 2001b):

$$\frac{\eta_{sp}}{C} = [\eta] + k_H [\eta]^2 C \quad \text{Eq. 2}$$

### 2.5.3. Steady shear properties

**2.5.3.1. Time-independent properties.** The steady shear measurements were conducted using a rotational viscometer (DVR, USA) equipped with a heating circulator at 25 °C to control desired temperature. Appropriate spindle was selected based on the solutions viscosity. The steady shear flow properties of MOSG solutions were determined by the Power-law equation:

$$\tau = k\dot{\gamma}^n \quad \text{Eq. 3}$$

here,  $\tau$ ,  $\dot{\gamma}$ ,  $k$  and  $n$  represent the shear stress (Pa), shear rate (s<sup>-1</sup>), consistency coefficient (Pa s<sup>n</sup>) and flow behavior index (dimensionless), respectively.

**2.5.3.2. Time-dependent properties.** Before evaluation of the time-dependent behavior, the gum solutions were subjected to a constant value of shear rate. The MOSG solutions with various concentrations (0.5, 1 and 1.5% (w/v)) were sheared at 50 s<sup>-1</sup>. The values of shear stress and apparent viscosity against time of shearing were plotted.

Following models were used to describe the time-dependent properties of the gum solutions:

Weltman model:

$$\tau = A + B \ln t \quad \text{Eq. 4}$$

where,  $\tau$ ,  $A$  and  $B$  are shear stress, initial shear stress and the time coefficient of thixotropic structure.

First-order stress decay model:

$$\tau - \tau_{eq} = (\tau_0 - \tau_{eq})e^{-kt} \quad \text{Eq. 5}$$

in which,  $\tau_0$ ,  $\tau_{eq}$  and  $k$  are initial shear stress, equilibrium shear stress and breakdown rate constant, respectively.

## 2.6. Zeta potential measurement

The zeta potential of the gum was determined using dynamic light scattering (DLS). For this purpose, the gum solution (0.1% v/v) was prepared and the surface charge of MOSG macromolecules was evaluated according to the electrophoretic mobility.

## 2.7. Surface tension measurement

The surface-tension measurement was conducted at 24 °C using Data Physics OCA15 plus tensiometer as described by Grein et al. (2013).

## 2.8. Molecular weight determination

Molecular weight properties and molecular homogeneity of MOSG were evaluated by a gel permeation chromatography (GPC), fitted by a PL Aquagel-OH Mixed-H column. The signals were detected by a refractive index (RI) detector. Deionized water was used as mobile phase at a constant flow rate of 1 mL/min. The column was calibrated by dextran with a range of molecular weight between 5200 and 988000 g/mol. The measurement was performed at 25 °C.

## 2.9. Statistical analysis

The experiments were conducted in triplicate. The data obtained from rheological evaluation were analyzed by one-way analysis of variance (ANOVA) using SPSS 16 (SPSS Inc., Chicago, IL). Duncan's multiple range test was employed to compare the treatments.

## 3. Results and discussions

### 3.1. Chemical composition

The total carbohydrate, moisture, ash and protein contents, monosaccharide constituent and mineral profile of MOSG are given in Table 1. The total carbohydrate content (TCC) of the gum was found to be 86.85% (w/w). Comparatively, TCC of MOSG was higher than those reported for commercial gums such as guar gum (71.1%) and gum ghatti (78.365), and was close to that registered for locust bean gum (85.1–88.7%) (Busch, Kolender, Santagapita, & Buera, 2015; Dakia, Blecker, Robert, Wathelet, & Paquot, 2008; Kang et al., 2011). Various factors such as TCC, molecular weight, monosaccharide composition and glycosides linkage can affect the stabilizing and gelling abilities of hydrocolloids. Since MOSG had high amount of TCC, it is expected that this gum can be used as an effective stabilizer in food systems. However, further analyses should be performed to confirm it. It was observed that TCC of MOSG obtained by phenol-sulfuric acid assay (86.85%) was slightly greater than that obtained by the subtraction of 100 from the

sum of moisture, protein, ash and fat contents (84.88%). This observation is consistent with that reported for *Lallemantia iberica* seed gum (Fathi et al, 2018). The reason for that has been related to incomplete ashing of the samples at 550 °C for 3 h.

Since the monosaccharide composition of hydrocolloids has considerable effect on their functional properties, the monosaccharide constituent of MOSG was determined (Table 1). The results revealed that MOSG is mainly composed of galactose and mannose.

Uronic acid content of MOSG (19.66%) was higher than those of some commercial hydrocolloids such as arabic gum (15.0%) and gum ghatti (12.38%), and was close to the value reported for xanthan gum (21.9%) (Anderson, Douglas, Morrison, & Weiping, 1990; Cui & Mazza, 1996; Kang et al., 2011). The uronic acid content in gums is a measure of the relative acidity. Thus, MOSG is a polysaccharide with high acidic nature. From a structural perspective, uronic acids are composed of acidic groups such as carbonyl and carboxylic acid that control the electrostatic interaction strength. At a pH below the acid dissociation constant of uronic acid, carbonyl and carboxylic acid groups of uronic acids will be in deprotonated form, making possible that the macromolecules be bonded with positively charged ions/polymers through electrostatic interactions. The resulting complex can be used as a carrier for encapsulation of ingredients (Fathi, Emam-Djomeh, & Aliabbasi, 2021). As mentioned above, MOSG is a highly acidic polysaccharide and thus can be used for encapsulation of phytochemicals using electrostatic interactions.

The protein content of MOSG was 0.90% which is lower than most of hydrocolloids, confirming again the high purity of this gum. It has been proved that proteins can avoid the coalescence and flocculation of oil droplets (Tomás, Bosquez-Molina, Stolik, & Sánchez, 2005). Furthermore, the role of proteins, as stabilizing agent for foams has been broadly reported (Das and Kinsella, 1990; Lusk et al, 1995; Marinova et al., 2009). Accordingly, MOSG might be used as stabilizer in many food systems; however, further testes should be carried out for better understanding the stabilizing ability of MOSG in food systems.

The moisture content of MOSG was 8.22%. It has been reported that if the moisture content of gums be lower than 15.0%, their quality preserve during storage period (Malsawmtluangi et al., 2014). Therefore, it is expectable that the quality of MOSG will preserve after storage.

Ash content of MOSG was found to be 6.00% which was considerably higher than that cited for locust bean gum (0.7–1.5%), but was lower than the data reported for guar gum (11.9%) (Cui & Mazza, 1996; Dakia et al., 2008). High value of ash in MOSG encouraged us to elucidate the mineral profile of this gum. As presented in Table 1, MOSG had high content of nutritional elements and therefore, can be suggested as a viable candidate for applying as a nutritional additive in the food systems.

The content of phenol compound in MOSG composition was found to be 49.43 ± 0.09 mg/g dry, as gallic acid, which was comparable to the data reported for hsian-tsoo leaf gum (43.47 mg/g dry, as gallic acid) (Lai, Chou, & Chao, 2001). Based on literature, phenolic compound can interact with free radicals (Bashi, FazlyBazzaz, Sahebkar, Karimkhani, & Ahmadi, 2012). Thus, MOSG can be suggested as a viable alternative for synthetic antioxidants.

### 3.2. FT-IR and NMR spectroscopy

In the present study, FT-IR and NMR (<sup>13</sup>C) analyses were conducted to elucidate the structure of MOSG. From the FTIR spectrum of MOSG (Fig. 1), different signals are detectable.

The signals detected in the range of 400 cm<sup>-1</sup> and 700 cm<sup>-1</sup> are related to the skeleton vibration of polysaccharides. The diagnostic signals in finger print area for carbohydrates (800–1200 cm<sup>-1</sup>) are 898.52, 1035.24 and 1149.32 cm<sup>-1</sup>. In this region, the wavenumber around 898.52 cm<sup>-1</sup> is attributed to α and β linkages in the gum structure. The absorbance at 820 cm<sup>-1</sup> indicated the presence of mannose in MOSG structure (Chen, Zhang, Jiang, Mu, & Miao, 2012). The peaks at

**Table 1**  
Proximate analysis and monosaccharide composition of MOSG.

Composition (%)	MOSG
Carbohydrate	86.85 ± 3.17
Protein	0.90 ± 0.08
Ash	6.00 ± 0.30
Moisture	8.22 ± 0.24
Fat	MDL <sup>a</sup>
<b>Monosaccharides</b>	
Arabinose	9.5 ± 0.9
Galactose	68.6 ± 3.6
Xylose	1.1 ± 0.1
Mannose	20.0 ± 2.9
Rhamnose	0.8 ± 0.1
Arabinose	
<b>Elements (ppm)</b>	
Calcium (Ca)	7071.3 ± 55.9
Magnesium (Mg)	2829.7 ± 29.6
Manganese (Mn)	51.84 ± 0.5
Potassium (K)	10994.4 ± 168.4
Phosphorus (P)	724.8 ± 6.4
Copper (Cu)	149.4 ± 1.4
Nickel (Ni)	8.84 ± 0.0
Sodium (Na)	2657.2 ± 37.9
Arsenic (As)	<MDL

<sup>a</sup> Method Detection Limit.

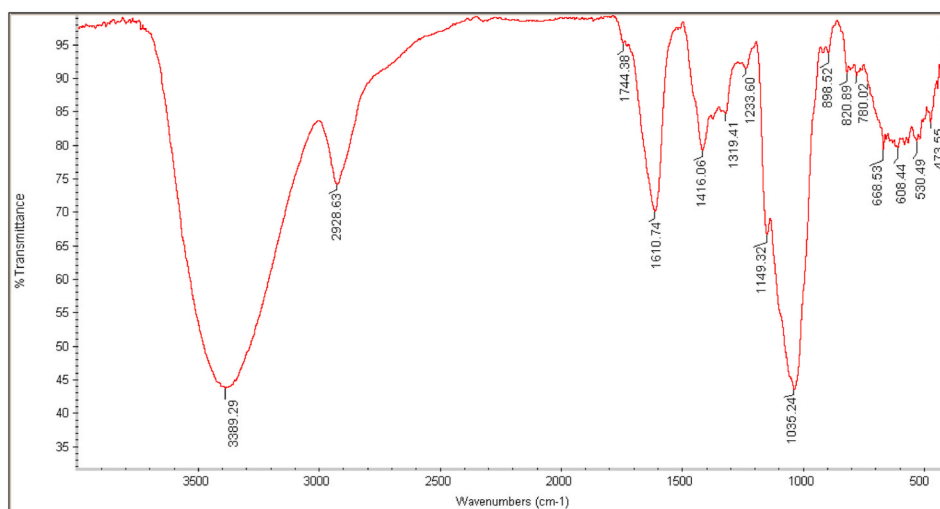


Fig. 1. FT-IR spectrum of MOSG.

1035.24 is arise from the presence of uronic acids in MOSG structure (Percival & Percival, 1962). The presence of uronic acid indicates that MOSG has an anionic nature. The peaks detected in the wavenumber range of  $1200\text{ cm}^{-1}$  to  $1500\text{ cm}^{-1}$  are associated with coupling of the deformation vibrations of groups consisting of hydrogen atoms (Vanloot, Dupuy, Guiliano, & Artaud, 2012). In the spectrum of MOSG, three bonds ( $1233.60$ ,  $1319.41$  and  $1416.06\text{ cm}^{-1}$ ) were observed in this region. The signal at  $1416.41\text{ cm}^{-1}$  and  $1610.74\text{ cm}^{-1}$  correspond to symmetric stretching vibration of  $\text{COO}^-$ . Carboxyl groups in the structure of polysaccharides can be deprotonated when the pH increased up to acid association constant. In this condition, carboxyl groups interact with positive cations and produce coacervate. The coacervate can entrap phytochemicals to preserve them against adverse environmental and physiological conditions.

The peak detected at  $2928\text{ cm}^{-1}$  is due to the stretching vibration of C-H in a methylene group ( $\text{CH}_2$ ) (Kacurakova, Capek, Sasinkova, Wellner, & Ebringerova, 2000). The absorbance between  $3100$  and  $3500\text{ cm}^{-1}$  is related to hydroxyl groups.

Before NMR analysis, the MOSG powder was diluted by  $\text{D}_2\text{O}$  to obtain sharp peaks and improve the quality of spectra.  $^{13}\text{C}$  NMR spectrum of MOSG is presented in Fig. 2. The resonance at  $\delta 16.51\text{ ppm}$  is assigned to C-6 methyl group of rhamnose. The signals of carbon atoms having primary hydroxyl groups, such as C-6 in pyranoses and C-5 in furanoses, will appear at a higher field of  $60\text{--}64\text{ ppm}$ , whereas the signals of carbon atoms with secondary hydroxyl groups (C2,3,4 in

pyranoses and C2,3 in furanoses) will appear in the region of  $65\text{--}87\text{ ppm}$ . The signal detected at around  $60\text{ ppm}$  may be related to  $\beta\text{-D-mannopyranosyl}$  (C-6) and the peak at  $68.38\text{ ppm}$  is due to  $\beta\text{-D-mannopyranosyl}$  (C-2) (Thambiraj, Phillips, Koyyalamudi, & Reddy, 2018). The diagnostic signals around  $72$  and  $73\text{ ppm}$  are attributed to C-2 and C-4 of  $\alpha\text{-D-galactopyranosyl}$ , respectively. The peaks diagnosed at  $\delta 79.77\text{--}83.50$  are associated with C-2 of  $\alpha\text{-L-Araf}$  units (Bock & Pedersen, 1984; Gorin & Mazurek, 1975; Tischer, Iacomini, Wagner, & Gorin, 2002). The signal at  $96.78\text{ ppm}$  is assigned to  $\beta\text{-D-mannopyranosyl}$  (C-1) (Thambiraj et al., 2018).

The observed signals at  $\delta 109.51\text{ ppm}$  corresponds to  $\alpha\text{-L-Araf}$  units (Delgobo, Gorin, Tischer, & Iacomini, 1999). The signals at  $\delta 101.17$ ,  $\delta 102.59$  and  $\delta 103.06\text{ ppm}$  are related to  $1\rightarrow 3$ -linked  $\beta\text{-D-Galp}$ ,  $\beta\text{-D-Xylp}$ , and  $1\rightarrow 4\text{-}\alpha\text{-Galp}$  unites, respectively (de Pinto, Martinez, de Corredor, Rivas, & Ocando, 1994; Fathi, Mohebbi, & Koocheki, 2016). The signal at  $\delta 175.9\text{ ppm}$  is attributed to carbonyl groups of the terminal non-reducing  $\text{D-glucuronic acid}$  (Rezagholi et al., 2019).

### 3.3. Molecular weight properties and rheological behavior

The molecular weight has considerable effect on thickening and gelling properties of polymers. Furthermore, this parameter can change the structure of fibrous produced by electrospinning technique (Abazović et al., 2006). It also has been reported that molecular weight affects the functional properties of hydrocolloids (Yang, Jiang, Zhao,

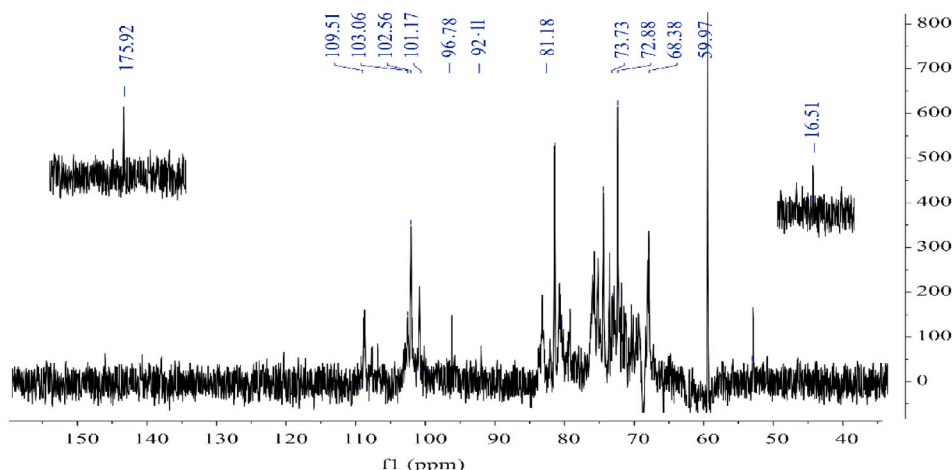


Fig. 2.  $^{13}\text{C}$  NMR of MOSG

Shi, & Wang, 2008). Hence, in the present work, the macromolecular properties of MOSG were evaluated to elucidate its potential applications in food systems. The weight ( $M_w$ ) and number ( $M_n$ ) average molecular weights and polydispersity index ( $PDI = M_w/M_n$ ) of MOSG were found to be  $1.36 \times 10^7$  g/mol,  $5.60 \times 10^6$  g/mol, and 2.43, respectively.

The GPC profile of MOSG is presented in Fig. 3. A large symmetric peak and two very small peaks were detected in GPC profile of the polysaccharide, revealing a low degree of homogeneity for MOSG. The major peak was used to determine the molecular weight of MOSG.

Mw of MOSG was  $1.36 \times 10^7$  g/mol, which is greater than those of commercial gums. Accordingly, it is expected that MOSG can be employed as a good thickener. However, further experiments like rheological analysis should be performed to confirm this result.

Rheological behavior of MOSG solutions in two different regimes (dilute solution and steady-state) were evaluated.

Intrinsic viscosity, as a physical property is mainly dependent on the quality of solvent, macromolecular structure, and molecular weight. The first step for estimation of intrinsic viscosity is distinguishing the dilute region. For this purpose, the values of relative viscosity ( $\eta_{rel}$ ) against polymer concentration were plotted. The coil-overlap point, where macromolecular entanglements begin, was about 0.34 g/dL. Accordingly, the intrinsic viscosity was determined below this point. The adequacies of the model were tested by the values of determination coefficient ( $R^2$ ), Adj- $R^2$  and root mean square error. Huggins model had high values of coefficient of determination ( $R^2$ ) and Adjusted- $R^2$  and minimum value of root mean square error (RMSE), indicating this model can be employed to describe the dilute solution properties MOSG. The intrinsic viscosity of MOSG was 3.45 dL/g, which was greater than arabic gum (0.6 dL/g) (Mothe & Rao, 1999), and lower than those reported for guar gum (9.25 dL/g) (Richardson, Willmer, & Foster, 1998), and lower than the value reported for Tragacanth (19.2 dL/g) (Mohammadifar, Musavi, Kiumarsi, & Williams, 2006).

Huggins constant can be used to evaluate the solvent quality. For instance, for a flexible molecule with an extended shape in the good solvent, the value of Huggins constant is in the range of 0.3–0.4. The values of this parameter for MOSG was calculated to be 0.32, revealing that deionized water is a good solvent for this biopolymer.

The plot of shear stress versus shear rate for MOSG solutions at various concentrations is given in Fig. 4. With increasing shear rate, the apparent viscosity (the slope of curve) decreased, demonstrating a shear-thinning behavior for the gum solutions. With increase of shear rate, the macromolecular chains are rearranged in the direction of flow, and consequently the interaction between chains reduced. This phenomena leads to decrease of viscosity (Marcotte et al, 2001). Furthermore, this observation has been related to the decrease in the number of chain entanglements (Nehdi, 2011). On the other hand, following an increase in gum concentration, apparent viscosity showed an increasing trend. This effect is due to the higher solid contents at higher concentration, which resulted in increasing macromolecular entanglements, in

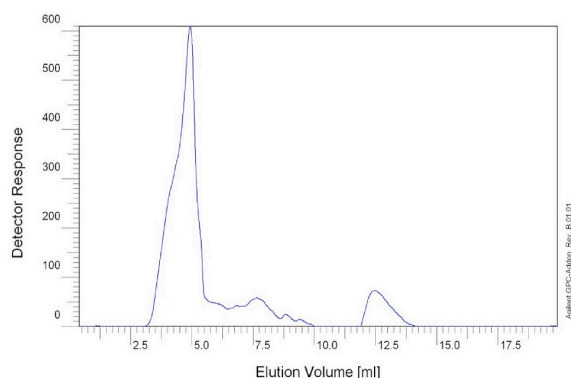


Fig. 3. GPC graph of MOSG.

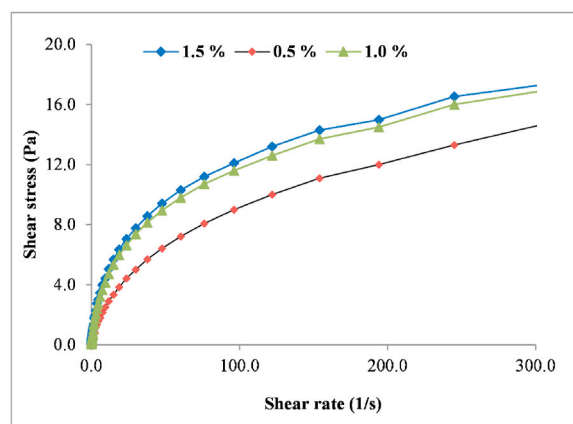


Fig. 4. Viscosity-shear rate profile of MOSG as a function concentration.

turn, improving the apparent viscosity (Maskan & Gogus, 2000).

In order to describe the time-dependent behavior of MOSG solution, Weltman and First-order stress decay models were used. From the data given in Table 2, it is evident that Weltman is the best model for describing the rheological data. This model has also been suggested as a suitable model to describe the time-dependency of some food products like salad dressings (PAREDES et al, 1988), fruit jams (Carbonell et al, 1991) and yogurt (O'Donnell & Butler, 2002).

The parameters obtained from Weltman model changed with increasing gum concentration. B value is an indicator for the extent of thixotropy. A negative value of B parameter was obtained for MOSG at tested concentrations, demonstrating a thixotropic behavior. An increase in gum concentration was accompanied by an increase in B value, indicating a greater thixotropic behavior at higher concentration.

### 3.4. Surface charge and particle size of MOSG molecules

The surface charge of biopolymers has an important factor in their utilization as carrier in encapsulation of ingredient by coacervation technique. Furthermore, zeta potential of biopolymers is considered as a key role in producing fibrous by electrospinning. The zeta potential of MOSG was found to be  $-44.26 \pm 0.67$  mV (at pH = 7). Accordingly, MOSG is an anionic biopolymer which is correlated with those observed by FT-IR analysis described above. Comparatively, the surface charge of MOSG is close to that reported for *Lepidium perfoliatum* seed gum ( $-43.7$  mV) (Soleimanpour et al, 2013) and greater than those of peach gum ( $-20$  mV) (Huang & Zhou, 2014) and *Alyssum homolocarpum* seed gum ( $-25.81$  mV) (Hesarinejad et al, 2015).

Since the particle size of polymers can affect their gelling ability, the determination of particle size of polymer is useful in predicting their rheological properties. Furthermore, the powder flow-ability is profoundly affected by the particle size (Liu et al., 2008). The powder flow-ability improves by increasing particle size. The particle size of MOSG powder was, on average,  $3461 \pm 48$  nm, which was lower than

Table 2

The parameters obtained from Weltman and First-order stress decay models.

Gum conc (%)	Weltman model			$R^2$	Adj- $R^2$
	A (Pa.s)	-B (Pa)	-		
0.5	65.2	3.2	-	0.97	0.96
1	76.9	5.8	-	0.95	0.93
1.5	114.5	8.9	-	0.95	0.92
	First-order stress decay model				
	$\tau_0$ (Pa)	$\tau_{eq}$ (Pa)	$k \times 10^{-3}$	$R^2$	Adj- $R^2$
0.5	52.4	41.3	8.2	0.84	0.79
1	59.63	46.6	9.3	0.81	0.76
1.5	102.3	49.1	9.0	0.81	0.76

that of food grade guar gum (54–500  $\mu\text{m}$ ). Thus, it is expected that this gum impart high viscosity to solvent, which was discussed above.

### 3.5. Surface tension

The surface tension of MOSG solutions at various concentrations is presented in Fig. 5. The decrease in surface tension is concentration-dependent: with increasing gum concentration from 0.01 to 0.5%, the surface tension of the samples decreased from 86.00 to 79.23 mN/m, but with further increasing gum concentration, surface tension of the solution increased. This trend is consistent with those observed for most of gums. Chaires-Martínez, Salazar-Montoya, and Ramos-Ramírez (2008) indicated that surface tension of locust bean gum decreased with increasing the concentration from 0.1 to 0.3%, but it increased at higher gum concentration. Razavi, Cui, Guo, and Ding (2014) also reported that an increase in sage seed gum concentration from 0.01 to 0.25% led to a decrease in surface tension, but it increased at higher concentration. The increment of surface tension at high concentration could be attributed to the excessive development of viscosity, which made surface tension determination difficult (Brummer et al., 2003). The surface activity of the gums could arise from the presence of hydrophobic functional groups (acetyl and methoxy groups), proteins and fractions with small molecular weight (Brummer et al., 2003; Dickinson, 2003) which were confirmed by FT-IR and compositional analyses described above. Comparatively, the surface activity of MOSG in a concentration of 0.5% (w/v) (~81 dyn/cm) was lower than those reported for fenugreek gum (50.3 dyn/cm), xanthan (60.8 dyn/cm), and arabic gum (46.9 dyn/cm) (Huang et al., 2001a, 2001b). The gum dispersions with lower surface activity have better wetting ability and therefore, results in formation of granules with higher quality (Farooq, Sharma, & Malviya, 2014). Generally, it can be proposed that MOSG gum can be used in oil/water emulsions due its ability to reduce surface tension.

### 3.6. Antioxidant activity

Based on available literature, polysaccharides have antioxidant activity that can be evaluated by different techniques like free radical compound DPPH. In the present work, we evaluated the DPPH radical scavenging effect of MOSG solutions with various concentrations.

The DPPH radical scavenging activity is broadly employed to determine the ability of gums and mucilages to scavenge free radicals (Abazović et al., 2006). The capacity of MOSG and butylated hydroxytoluene (BHT) solutions to inhibit free DPPH radicals as a function of concentration is depicted in Fig. 6. As expected, following an increase in MOSG concentration, the radical scavenging effect increased, showing an electron-donating ability for MOSG. The same observations have been reported by other researchers (Dokht et al., 2018; Malsawmtluangi et al., 2014; Pu et al., 2016). This effect has been related to the interaction between polysaccharides with free radical, which leads to production of the products with high stability. Similarly, when BHT concentration increased, the radical scavenging effect increased. The radical scavenging effect of MOSG solutions were slightly lower than that observed for BHT ( $\text{IC}_{50}$  of MOSG and BHT were found to be 62.3 and 47.4  $\mu\text{g}/\text{mL}$ , respectively). Furthermore, the radical scavenging effect of this gum was greater than those of natural polymers like *Albizia stipulate* and *Prunus cerasoides* gums (Malsawmtluangi et al., 2014; Thanzami et al., 2015).

## 4. Conclusion

The results of the present work indicated that MOSG is a heterogenic polysaccharide composed of 86.85 % carbohydrate. The monosaccharides present in the gum composition are galactose (68.6 %), arabinose (9.5 %), xylose (1.1 %), and mannose (20.0 %). MOSG had high molecular weight with a heterogenic GPC profile. High viscosifying ability of this gum indicated that MOSG can be used as thickener in

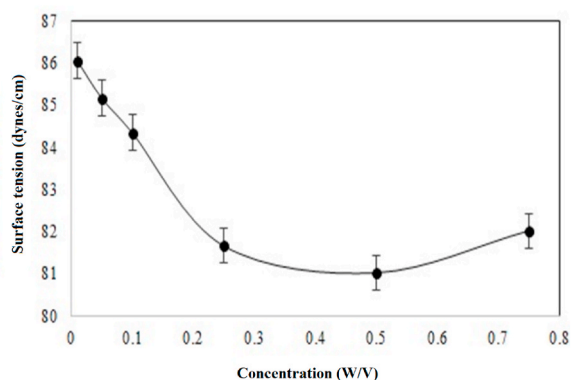


Fig. 5. The surface activity of MOSG as a function concentration.

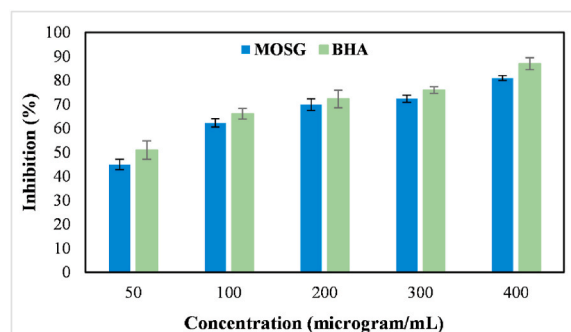


Fig. 6. DPPH antiradical activity of MOSG as a function of concentration.

drinks and beverages. MOSG solutions exhibited time-dependent thixotropic behavior. Weltman model was the best models to describe the time-dependent behavior of MOSG solutions. MOSG showed an excellent ability to scavenge free radicals.

### Data availability

Data available on request due to privacy/ethical restrictions

### CRediT authorship contribution statement

**Mohebbat Mohebbi:** Supervision, Writing – review & editing. **Morteza Fathi:** Investigation, Writing – original draft, Methodology, Software. **Mohammad Khalilian-Movahhed:** Investigation, Writing – original draft, Software.

### Declaration of competing Interest

We declare that there are no conflict of interest.

### Acknowledgements

Financial support was granted by Ferdowsi University of Mashhad (Funder's Grant Number: 1/40018)

### References

- Abazović, N. D., Čomor, M. I., Dramićanin, M. D., Jovanović, D. J., Ahrenkiel, S. P., & Nedeljković, J. M. (2006). Photoluminescence of anatase and rutile TiO<sub>2</sub> particles. *The Journal of Physical Chemistry B*, 110(50), 25366–25370.
- Anderson, D., Douglas, D. B., Morrison, N., & Weiping, W. (1990). Specifications for gum arabic (*Acacia Senegal*); analytical data for samples collected between 1904 and 1989. *Food Additives & Contaminants*, 7(3), 303–321.

- Andres, K., Von Düring, M., Muszynski, K., & Schmidt, R. (1987). Nerve fibres and their terminals of the dura mater encephali of the rat. *Anatomy and embryology*, 175(3), 289–301.
- Bashi, D. S., Fazly Bazzaz, B. S., Sahebkar, A., Karimkhani, M. M., & Ahmadi, A. (2012). Investigation of optimal extraction, antioxidant, and antimicrobial activities of *Achillea biebersteinii* and *A. wilhelmsii*. *Pharmaceutical Biology*, 50(9), 1168–1176.
- Blois, M. S. (1958). *Antioxidant determinations by the use of a stable free radical*.
- Bock, K., & Pedersen, H. (1984). Assignment of the NMR Parameters of the branch-Point trisaccharide of ahylopectin Using 2-D NMR Spectroscopy at 500 MHz. *Journal of Carbohydrate Chemistry*, 3(4), 581–592.
- Bradford, M. M. (1976). A rapid and sensitive method for the quantitation of microgram quantities of protein utilizing the principle of protein-dye binding. *Analytical biochemistry*, 72(1-2), 248–254.
- Brunner, Y., & Cui, S. W. (2005). Understanding carbohydrate analysis. *Food carbohydrates: chemistry, physical properties and applications*, 1–38.
- Brunner, Y., Cui, W., & Wang, Q. (2003). Extraction, purification and physicochemical characterization of fenugreek gum. *Food Hydrocolloids*, 17(3), 229–236.
- Busch, V., Delgado, J., Santagapita, P., Wagner, J., & Buera, M. (2018). Rheological characterization of vinal gum, a galactomannan extracted from *Prosopis ruscifolia* seeds. *Food Hydrocolloids*, 74, 333–341.
- Busch, V. M., Kolender, A. A., Santagapita, P. R., & Buera, M. P. (2015). Vinal gum, a galactomannan from *Prosopis ruscifolia* seeds: Physicochemical characterization. *Food Hydrocolloids*, 51, 495–502.
- Carbonell, E., Costell, E., & Duran, L. (1991). Rheological indices of fruit content in jams: Influence of formulation on time-dependent flow of sheared strawberry and peach jams. *Journal of Texture Studies*, 22(4), 457–471.
- Chaires-Martínez, L., Salazar-Montoya, J., & Ramos-Ramírez, E. (2008). Physicochemical and functional characterization of the galactomannan obtained from mesquite seeds (*Prosopis pallida*). *European Food Research and Technology*, 227(6), 1669.
- Chen, J., Zhang, T., Jiang, B., Mu, W., & Miao, M. (2012). Characterization and antioxidant activity of Ginkgo biloba exocarp polysaccharides. *Carbohydrate Polymers*, 87(1), 40–45.
- Cui, W., & Mazza, G. (1996). Physicochemical characteristics of flaxseed gum. *Food Research International*, 29(3), 397–402.
- Dakia, P. A., Blecker, C., Robert, C., Wathelet, B., & Paquot, M. (2008). Composition and physicochemical properties of locust bean gum extracted from whole seeds by acid or water dehulling pre-treatment. *Food Hydrocolloids*, 22(5), 807–818.
- Das, K., & Kinsella, J. (1990). *Stability of food emulsions: Physicochemical role of protein and nonprotein emulsifiers. Advances in food and nutrition research* (Vol 34, p. 81). Elsevier.
- Delgado, C. L., Gorin, P. A., Tischer, C. A., & Iacomini, M. (1999). The free reducing oligosaccharides of angico branco (anadenantheracolubrina) gum exudate: An aid for structural assignments in the heteropolysaccharide. *Carbohydrate Research*, 320(3–4), 167–175.
- Dickinson, E. (2003). Hydrocolloids at interfaces and the influence on the properties of dispersed systems. *Food Hydrocolloids*, 17(1), 25–39.
- Dokht, S. K., Djomeh, Z. E., Yarmand, M. S., & Fathi, M. (2018). Extraction, chemical composition, rheological behavior, antioxidant activity and functional properties of *Cordia myxa* mucilage. *International Journal of Biological Macromolecules*, 118, 485–493.
- Farooq, U., Sharma, K., & Malviya, R. (2014). Extraction and characterization of almond (*Prunus dulcis*) gum as pharmaceutical extract. *American-Eurasian Journal of Agricultural & Environmental Sciences*, 14, 269–274.
- Fathi, M., Emam-Djomeh, Z., & Aliabassi, N. (2021). Developing two new types of nanostructured vehicles to improve biological activity and functionality of curcumin. *Food Bioscience*, 44, 101386.
- Fathi, M., Emam-Djomeh, Z., & Sadeghi-Varkani, A. (2018). Extraction, characterization and rheological study of the purified polysaccharide from *Lallemantia ibricea* seeds. *International Journal of Biological Macromolecules*, 120, 1265–1274.
- Fathi, M., Mohebbi, M., & Koocheki, A. (2016). Introducing *Prunus cerasus* gum exudates: Chemical structure, molecular weight, and rheological properties. *Food Hydrocolloids*, 61, 946–955.
- Gorin, P. A., & Mazurek, M. (1975). Further studies on the assignment of signals in <sup>13</sup>C magnetic resonance spectra of aldoses and derived methyl glycosides. *Canadian Journal of Chemistry*, 53(8), 1212–1223.
- Grein, A., da Silva, B. C., Wendel, C. F., Tischer, C. A., Sierakowski, M. R., Moura, A. B. D., et al. (2013). Structural characterization and emulsifying properties of polysaccharides of *Acacia mearnsii* de Wild gum. *Carbohydrate Polymers*, 92(1), 312–320.
- Hesarinejad, M., Razavi, S. M., & Koocheki, A. (2015). *Alyssum homolocarpum* seed gum: Dilute solution and some physicochemical properties. *International Journal of Biological Macromolecules*, 81, 418–426.
- Huang, X., Kakuda, Y., & Cui, W. (2001a). Hydrocolloids in emulsions: Particle size distribution and interfacial activity. *Food Hydrocolloids*, 15(4–6), 533–542.
- Huang, X., Kakuda, Y., & Cui, W. (2001b). Hydrocolloids in emulsions: Particle size distribution and interfacial activity. *Food Hydrocolloids*, 15(4), 533–542.
- Huang, J., & Zhou, L. (2014). Peach gum polysaccharide polyelectrolyte: Preparation, properties and application in layer-by-layer self-assembly. *Carbohydrate Polymers*, 113, 373–379.
- International, A. (2005). *Official methods of analysis of AOAC International*. AOAC International.
- Kacurakova, M., Capek, P., Sasinkova, V., Wellner, N., & Ebringerova, A. (2000). FT-IR study of plant cell wall model compounds: Pectic polysaccharides and hemicelluloses. *Carbohydrate Polymers*, 43(2), 195–203.
- Kang, J., Cui, S. W., Chen, J., Phillips, G. O., Wu, Y., & Wang, Q. (2011). New studies on gum ghatti (*Anogeissus latifolia*) part I. Fractionation, chemical and physical characterization of the gum. *Food Hydrocolloids*, 25(8), 1984–1990.
- Lai, L.-S., Chou, S.-T., & Chao, W.-W. (2001). Studies on the antioxidative activities of Hsian-tsoa (*Mesona procumbens* Hemsl.) leaf gum. *Journal of Agricultural and Food Chemistry*, 49(2), 963–968.
- Liu, L., Marziano, I., Bentham, A., Litster, J., White, E., & Howes, T. (2008). Effect of particle properties on the flowability of ibuprofen powders. *International Journal of Pharmaceutics*, 362(1), 109–117.
- Lusk, L. T., Goldstein, H., & Ryder, D. (1995). Independent role of beer proteins, melanoidins and polysaccharides in foam formation. *Journal of the American Society of Brewing Chemists*, 53(3), 93–103.
- Malsawmtluangi, C., Thanzami, K., Lahlhenmawia, H., Selvan, V., Palanisamy, S., Kandasamy, R., et al. (2014). Physicochemical characteristics and antioxidant activity of *Prunus cerasoides* D. Don gum exudates. *International Journal of Biological Macromolecules*, 69, 192–199.
- Marcotte, M., Hoshahili, A. R. T., & Ramaswamy, H. (2001). Rheological properties of selected hydrocolloids as a function of concentration and temperature. *Food Research International*, 34(8), 695–703.
- Marinova, K. G., Basheva, E. S., Nenova, B., Temelska, M., Mirarefi, A. Y., Campbell, B., et al. (2009). Physico-chemical factors controlling the foamability and foam stability of milk proteins: Sodium caseinate and whey protein concentrates. *Food Hydrocolloids*, 23(7), 1864–1876.
- Maskan, M., & Göğüş, F. (2000). Effect of sugar on the rheological properties of sunflower oil-water emulsions. *Journal of Food Engineering*, 43(3), 173–177.
- Mohammadifar, M. A., Musavi, S. M., Kiumarsi, A., & Williams, P. A. (2006). Solution properties of targacanthin (water-soluble part of gum tragacanth exudate from *Astragalus gossypinus*). *International Journal of Biological Macromolecules*, 38(1), 31–39.
- Mothe, C., & Rao, M. (1999). Rheological behavior of aqueous dispersions of cashew gum and gum Arabic: Effect of concentration and blending. *Food Hydrocolloids*, 13(6), 501–506.
- Nehdi, I. (2011). Characteristics, chemical composition and utilisation of *Albizia julibrissin* seed oil. *Industrial Crops and Products*, 33(1), 30–34.
- O'Donnell, H., & Butler, F. (2002). Time-dependent viscosity of stirred yogurt. Part I: Couette flow. *Journal of Food Engineering*, 51(3), 249–254.
- Paredes, M. D. C., Rao, M., & Bourne, M. C. (1988). Rheological characterization of salad dressings. 1. Steady shear, thixotropy and effect of temperature. *Journal of Texture Studies*, 19(3), 247–258.
- Percival, E. G. V., & Percival, E. (1962). *Structural carbohydrate chemistry*.
- de Pinto, G. L., Martínez, M., de Corredor, A. L., Rivas, C., & Ocando, E. (1994). Chemical and <sup>13</sup>C NMR studies of *Enterolobium cyclocarpum* gum and its degradation products. *Phytochemistry*, 37(5), 1311–1315.
- Pu, X., Ma, X., Liu, L., Ren, J., Li, H., Li, X., et al. (2016). Structural characterization and antioxidant activity in vitro of polysaccharides from angelica and astragalus. *Carbohydrate Polymers*, 137, 154–164.
- Razavi, S. M. A., Cui, S. W., Guo, Q., & Ding, H. (2014). Some physicochemical properties of sage (*Salvia macrosiphon*) seed gum. *Food Hydrocolloids*, 35, 453–462.
- Rezagholi, F., Hashemi, S. M. B., Gholamhosseinpour, A., Sherahi, M. H., Hesarinejad, M. A., & Ale, M. T. (2019). Characterizations and rheological study of the purified polysaccharide extracted from quince seeds. *Journal of the Science of Food and Agriculture*, 99(1), 143–151.
- Richardson, P. H., Willmer, J., & Foster, T. J. (1998). Dilute solution properties of guar and locust bean gum in sucrose solutions. *Food Hydrocolloids*, 12(3), 339–348.
- Singleton, V., & Rossi, J. A. (1965). Colorimetry of total phenolics with phosphomolybdenic-phosphotungstic acid reagents. *American Journal of Enology and Viticulture*, 16(3), 144–158.
- Soleimanpour, M., Koocheki, A., & Kadkhodae, R. (2013). Effect of *Lepidium perfoliatum* seed gum addition on whey protein concentrate stabilized emulsions stored at cold and ambient temperature. *Food Hydrocolloids*, 30(1), 292–301.
- Thambiraj, S. R., Phillips, M., Koyyalamudi, S. R., & Reddy, N. (2018). Yellow lupin (*Lupinus luteus* L.) polysaccharides: Antioxidant, immunomodulatory and prebiotic activities and their structural characterisation. *Food Chemistry*, 267, 319–328.
- Thanzami, K., Malsawmtluangi, C., Lahlhenmawia, H., Seelan, T. V., Palanisamy, S., Kandasamy, R., et al. (2015). Characterization and in vitro antioxidant activity of *Albizia stipulata* Boiv. gum exudates. *International Journal of Biological Macromolecules*, 80, 231–239.
- Tischer, C. A., Iacomini, M., Wagner, R., & Gorin, P. A. (2002). New structural features of the polysaccharide from gum ghatti (*Anogeissus latifolia*). *Carbohydrate Research*, 337(21–23), 2205–2210.
- Tomás, S., Bosquez-Molina, E., Stolik, S., & Sánchez, F. (2005). Effects of mesquite gum-candelilla wax based edible coatings on the quality of guava fruit (*Psidium guajava* L.). In *Journal de Physique IV (proceedings)* (Vol 125, pp. 889–892). EDP sciences.
- Vanloot, P., Dupuy, N., Guiliano, M., & Artaud, J. (2012). Characterisation and authentication of *A. Senegal* and *A. seyal* exudates by infrared spectroscopy and chemometrics. *Food Chemistry*, 135(4), 2554–2560.
- Vogl, S., Picker, P., Mihaly-Bison, J., Fakhrudin, N., Atanasov, A. G., Heiss, E. H., et al. (2013). Ethnopharmacological in vitro studies on Austria's folk medicine—an unexplored lore in vitro anti-inflammatory activities of 71 Austrian traditional herbal drugs. *Journal of Ethnopharmacology*, 149(3), 750–771.
- Wang, F., Wang, W., Huang, Y., Liu, Z., & Zhang, J. (2015). Characterization of a novel polysaccharide purified from a herb of *Cynomorium songaricum* Rupr. *Food Hydrocolloids*, 47, 79–86.
- Yang, B., Jiang, Y., Zhao, M., Shi, J., & Wang, L. (2008). Effects of ultrasonic extraction on the physical and chemical properties of polysaccharides from longan fruit pericarp. *Polymer Degradation and Stability*, 93(1), 268–272.